行政院國家科學委員會專題研究計畫 成果報告

經由地下水傳輸之壓力波的共振
研究成果報告(精簡版)

計 畫 類 別 ： 個別型
計 畫 編 號 ： NSC 95-2221-E-002-420-
執 行 期 間 ： 95 年 08 月 01 日至 96 年 07 月 31 日
執 行 單 位 ： 國立臺灣大學土木工程學系暨研究所

計 畫 主 持 人 ： 黃良雄

計畫參與人員 ： 主持人：黃良雄
博士班研究生：郭遠錦

處 理 方 式 ： 本計畫可公開查詢

中 華 民 國 96 年 09 月 05 日

Proceedings of the Seventeenth (2007) International Offshore and Polar Engineering Conference
Lisbon, Portugal, July 1-6, 2007

ISBN 978-1-880653-68-5; ISBN 1-880653-68-0(Set); ISSN 1098-6189 (Set)

A Study on the Mechanism of Water Well Resonance Induced by Pre-earthquake Signals

C.H. Wang
Dept. of Civil Engrg., Natl. Taiwan Univ., Taipei, TAIWAN, China
L.H. Huang
Dept. of Civil Engrg. and Hydrotech Res. Inst., Natl. Taiwan Univ., Taipei, TAIWAN, China.

ABSTRACT

In this study, we analyze the physical mechanism of water well resonance induced by pre-earthquake signals. A weak pressure wave passing through the confined aquifer is considered as the incoming pre-earthquake signal. Since the porous skeleton is hard, this pressure wave is simply the limiting case of second kind of dilatational wave of poroelasticity. Because the driving signals of weak pre-earthquake pressure wave transmitting through confined aquifer are so weak that can hardly affect the solid skeleton we, believe a very possible reason for this is due to the effect of resonant amplification of free surface water waves in wells. The water inside the well is assumed to be incompressible, inviscid and irrotational while that outside the well is treated as porous-media fluid flow with rigid skeleton. The potential flow theory with small amplitude water wave and porous media flow following Darcy's law are adopted for waters inside and outside the well respectively. By using the regular perturbation expansion method based on a small gauge function k_0R (k_0 is the wavenumber, R is the well radius), the well-posed boundary-value-problem thus can be solved. It is found that the weak pre-earthquake longitudinal pressure wave is only a triggering mechanism for the resonance of transverse gravitational free surface water wave inside the well.

KEYWORDS: pre-earthquake signals; well; resonance; longitudinal wave; transverse waves.

INTRODUCTION

The problem of the response of groundwater induced by earthquake has been studied by many investigators. For example, Cooper et al. (1965) is a study on the response of well water to seismic waves, and Liu and Wen (1997) is the analysis of the long waves passing through aquifer. However, researches on the response of groundwater induced by weak pre-earthquake signals are rare.

There are evidences, indeed, that groundwater somehow is affected by very weak pre-earthquake signals. For example, one day before the drastic 921-earthquake at central Taiwan in 1999, pre-earthquake responses were observed in some water wells in Tsuo-Shui River water basin in central Taiwan. Because the driving signals of weak pre-earthquake pressure wave transmitting through confined aquifer are so weak that can hardly affect the solid skeleton we, believe a very possible reason for this is due to the effect of resonant amplification of free surface water waves in wells. Although unlike resonances driven by large energy such as Cooper et al. (1965) or conventional harbour resonance researches, the traditional resonance analyzing methods are still worth referring to for our present study.

In Cooper et al. (1965), the oscillation of water column in a well due to an incoming harmonic seismic wave is studied. This problem is similar to the well-known oscillating fluid in a U-tube of fluid mechanics (e.g. see Chapter 13 of Streeter and Wylie (1985)). This study is about the response of well water due to huge seismic wave but not weak pre-earthquake wave. Although the resonance phenomena is not discussed in Copper et al. (1965), the resonant effect of it can be easily obtained.

Harbour resonance is an important problem for harbour design. The famous " Merian's formula" is just the result of the resonant analysis of water wave which relates the unfavored harbour geometry to the designed wave. There are many investigations about harbour resonance, for example, McNown (1952), Mei (1989), etc. are theoretical studies, Chen and Mei (1974), Tsay and Liu (1983), etc. are numerical researches.

In this study, we'll refer to the aforementioned resonance studies and analyze the resonance of water in wells in response to weak pre-earthquake signal transmitting through confined aquifer. A weak pressure wave passing through the confined aquifer is considered as the incoming pre-earthquake signal. The water inside the well is assumed to be incompressible, inviscid and irrotational while that outside the well is treated as porous-media fluid flow with rigid skeleton. The potential flow theory with small amplitude water wave and porous media flow following Darcy's law are adopted for waters inside and outside the well respectively.

FORMULATION

Governing Equations of Fluid in Confined Aquifer

Based on Biot's theory of poroelasticity, for the skeleton of the porous aquifer being assumed rigid, and the water incompressible, the continuity equation and the momentum equation for water inside the aquifer are

$$\nabla \cdot \underline{V}_4 = 0 \tag{1}$$

$$0 = -\nabla p_4 + \rho \underline{g} - \frac{\mu n_0}{k_p} \underline{V} \tag{2}$$

where subscript 4 refers to the aquifer region as shown in Figure 1; $\underline{V}_4$ = velocity vector of water; p_4 = pressure of the fluid inside the aquifer; ρ = density of the fluid; μ = dynamic viscosity of fluid; n_0 and k = porosity and specific permeability of the aquifer, respectively.

The velocity potential ϕ_4 may be defined as

$$\underline{V}_4 = -\frac{\rho g k_p}{\mu n_0} \nabla \phi_4 = -K \nabla \phi_4 \tag{3}$$

where K = hydraulic conductivity, and then, the continuity equation becomes

$$\nabla^2 \phi_4 = 0 \tag{4}$$

and integrating (2) with respect to the vertical coordinate z, (2) becomes

$$p_4 = -\rho g \phi_4 - \rho g (z - H) \tag{5}$$

In the foregoing equations, z = vertical upward coordinate from the bottom of the well; and H = depth of undisturbed water in the well.

Governing Equations of Fluid in Well

It is quite reasonable that homogeneous water in the well is assumed to be incompressible, inviscid and irrotational; and the fluid domains of the present study are shown in Figure 1.

For regions (1) - (3), we let

$$\underline{V}_j = \nabla \phi_j, \qquad j = 1,2,3 \tag{6}$$

where $\underline{V}_j$ and ϕ_j = velocity vectors and velocity potentials of fluid, respectively; and the subscript j denotes the flow regions (see Figure 1). The continuity equation and linear momentum equation are

$$\nabla \cdot \underline{V}_j = 0, \qquad j = 1,2,3 \tag{7}$$

$$\rho \frac{\partial \underline{V}_j}{\partial t} = -\nabla p_j + \rho \underline{g}, \qquad j = 1,2,3 \tag{8}$$

By substituting (6) into (7), (7) becomes

$$\nabla^2 \phi_j = 0, \qquad j = 1,2,3 \tag{9}$$

Then, by substituting (6) into (8), and integrating (8) with respect to z, (8) becomes

$$p_j = -\rho \frac{\partial \phi_j}{\partial t} - \rho g (z - H), \quad j = 1,2,3 \tag{10}$$

where t = time; p_j = the pressure of the fluid in the well.

Boundary Conditions

On the bottom of the well (i.e. $z = 0$, $0 < r < R$), the normal velocity equals zero, i.e.,

$$\frac{\partial \phi_3}{\partial z} = 0 \tag{11}$$

On the free surface of fluid in the well, $z = H$, $0 < r < R$ for region (1), we have the conventional kinematic and dynamic boundary conditions as

$$\frac{\partial \phi_1}{\partial z} = \frac{\partial \eta}{\partial t} \tag{12}$$

$$\frac{\partial \phi_1}{\partial t} + g\eta = 0 \tag{13}$$

where R = radius of the well; η = the vertical deviation of water surface from the mean free surface. For convenience, we usually combine (12) with (13) to get rid of η as

$$\frac{\partial^2 \phi_1}{\partial t^2} + g \frac{\partial \phi_1}{\partial z} = 0 \tag{14}$$

On the upper and lower aquitard / aquifer interface (i.e. $R < r < \infty$, $z = h_2$, and $z = h_1$), the boundary condition is

$$\frac{\partial \phi_4}{\partial z} = 0 \tag{15}$$

On the lateral surfaces inside the well except the screen, the normal velocity equals zero, i.e., $r = R$; $h_2 < z < H$ for flow region 1, and $0 < z < h_1$ for flow region 3, we get

$$\frac{\partial \phi_1}{\partial r} = 0 \tag{17}$$

$$\frac{\partial \phi_3}{\partial r} = 0 \tag{18}$$

where h_2 and h_1 = the height of upper and lower aquitard / aquifer interface.

On the lateral screen surface inside the well (i.e. $r = R$, and $h_1 < z < h_2$), the continuity conditions of mass flux and pressure are considered. From Eqs. (3) and (6), we have

$$\frac{\partial \phi_2}{\partial r} = n_0 K \frac{\partial \phi_4}{\partial r} \tag{19}$$

and according to Eqs. (5) and (10), it is obtained that

$$-\frac{1}{g} \frac{\partial \phi_2}{\partial t} = \phi_4 \tag{20}$$

At the far field, $h_1 < z < h_2$ and $r \to \infty$, the radiation boundary condition is

$$\lim_{r \to \infty} \phi_4 \to outgoing \quad or \quad 0 \tag{21}$$

On the interface between two regions in the well, the artificial internal boundaries, the continuity conditions of mass flux and pressure shall be satisfied as follows:

$$\frac{\partial \phi_1}{\partial z} = \frac{\partial \phi_2}{\partial z} \tag{22}$$

$$\phi_1 = \phi_2 \tag{23}$$

for region 1 / region 2, and

$$\frac{\partial \phi_2}{\partial z} = \frac{\partial \phi_3}{\partial z} \tag{24}$$

$$\phi_2 = \phi_3 \tag{25}$$

for region 2 / region 3.

Regular Perturbation Expansions

Since the present study focuses on the problem of periodic linear water wave, we may introduce a time factor $e^{-i\omega t}$ into the time-dependent variables. We shall use the same notation as time-dependent variables discussed earlier to represent the following time-independent variables for simplicity, where ω is the angular frequency of weak incident pressure wave.

Eqs. (4) and (9), together with boundary conditions (11) and (14)-(25), form a complete boundary-value-problem. However, because K in (19) is much less than one, we may encounter a highly ill-conditioned system when solving undetermined coefficients by matrix. Hence, we have to further simplify the problem in order to solve it.

Notice that by referring to reasonable order of magnitude of each variable such as $k_p \sim 10^{-10} m^2$, $\lambda \sim 10^8 \, N/m^2$, ω ~ 10^0 s^{-1}, $\mu \sim 10^{-4} \, kg/m \cdot s$, and $R \sim 10^{-1} m$, we find

$$k_0 R \sim \left\{ \frac{2G + \lambda + \kappa / n_0}{(2G + \lambda)\kappa n_0} i\omega (F\mu n_0^2 / k_p) \right\}^{1/2} . R \sim \sqrt{\frac{\omega \mu}{\lambda k_p}} R << 1 \tag{26}$$

where κ = volume bulk modulus of water, G = Lame constant, and F = non-dimensional parameter, for rigid skeleton of the porous aquifer according to Huang and Song (1993). We thus may introduce

$$\varepsilon = k_0 R \sim \sqrt{\frac{\omega\mu}{\lambda k_p}} R \sim 10^{-2} << 1 \quad (27)$$

as a small parameter to be the gauge function for regular perturbation expansion, where k_0 = wavenumber of weak incident pressure wave (i.e. wavenumber of the limiting case of second kind of longitudinal wave of poroelasticity); λ = Lame constant of elasticity. Different from that for low frequency tsunami long wave in Liu and Wen (1997), referring to (26), this k_0 for pre-earthquake signal may give very small decay rate when the wave is short and skeleton is rigid.

Also notice that

$$O\left(\frac{K}{k_0 R}\right) = O\left(\frac{\rho g k_p / \mu n_0}{\sqrt{\omega\mu/\lambda k_p}\, R}\right) \sim O(1)$$

or

$$O(K) \sim O(k_0 R) \sim O(\varepsilon) \quad (28)$$

where $n_0 \sim 1$, $\rho \sim 10^3\ kg/m^3$, $g \sim 10^1\ kg \cdot m/s^2$.

Considering (28) for boundary condition (19), we then find that it is quite natural to introduce the regular perturbation expansions with the gauge function ε as

$$\phi_1 = \phi_1^1 \varepsilon + O(\varepsilon^2) \quad (29)$$

$$\phi_2 = \phi_2^1 \varepsilon + O(\varepsilon^2) \quad (30)$$

$$\phi_3 = \phi_3^1 \varepsilon + O(\varepsilon^2) \quad (31)$$

$$\phi_4 = \phi_I^0 + \phi_4^0 + \phi_4^1 \varepsilon + O(\varepsilon^2) \quad (32)$$

We shall expect ϕ_I^0 to represent the incident pressure wave, ϕ_4^0 to represent the reflection pressure wave within the confined aquifer, while ϕ_1^1, ϕ_2^1, ϕ_3^1 to be the first-order perturbation solutions inside the well.

Dividing Methods

Since in the boundary-vale-problem of region 2, there are too many non-homogeneous boundary conditions, the general solution cannot be obtained straightforwardly. Based on the superposition principle for linear problem, we can use the dividing method to solve the original boundary-value problem. By letting

$$\phi_j^1 = \tilde{\phi}_j^1 + \hat{\phi}_j^1, \quad j = 1,2,3 \quad (33)$$

then for $\tilde{\phi}_j^1$,

region 1

$$\nabla^2 \tilde{\phi}_1^1 = 0,\ 0 < r < R,\ h_2 < z < H \quad (34)$$

$$-\omega^2 \tilde{\phi}_1^1 + g \frac{\partial \tilde{\phi}_1^1}{\partial z} = 0,\ z = H,\ 0 < r < R \quad (35)$$

$$\frac{\partial \tilde{\phi}_1^1}{\partial z} = 0,\ z = h_2,\ 0 < r < R \quad (36)$$

$$\frac{\partial \tilde{\phi}_1^1}{\partial r} = 0,\ r = R,\ h_2 < z < H \quad (37)$$

region 2

$$\nabla^2 \tilde{\phi}_2^1 = 0,\ 0 < r < R,\ h_1 < z < h_2 \quad (38)$$

$$\frac{\partial \tilde{\phi}_2^1}{\partial z} = 0,\ z = h_2,\ 0 < r < R \quad (39)$$

$$\frac{\partial \tilde{\phi}_2^1}{\partial z} = 0,\ z = h_1,\ 0 < r < R \quad (40)$$

$$\frac{\partial \tilde{\phi}_2^1}{\partial r} = n_0 K \frac{\partial}{\partial r}(\phi_I^0 + \phi_4^0),\ r = R,\ h_1 < z < h_2 \quad (41)$$

region 3

$$\nabla^2 \tilde{\phi}_3^1 = 0,\ 0 < r < R,\ 0 < z < H \quad (42)$$

$$\frac{\partial \tilde{\phi}_3^1}{\partial z} = 0,\ z = h_1,\ 0 < r < R \quad (43)$$

$$\frac{\partial \tilde{\phi}_3^1}{\partial z} = 0,\ z = 0,\ 0 < r < R \quad (44)$$

$$\frac{\partial \tilde{\phi}_3^1}{\partial r} = 0,\ r = R,\ 0 < z < h_1 \quad (45)$$

For $\hat{\phi}_j^1$,

region 1

$$\nabla^2 \hat{\phi}_1^1 = 0,\ 0 < r < R,\ h_2 < z < H \quad (46)$$

$$-\omega^2 \hat{\phi}_1^1 + g \frac{\partial \hat{\phi}_1^1}{\partial z} = 0,\ z = H,\ 0 < r < R \quad (47)$$

$$\frac{\partial \hat{\phi}_1^1}{\partial z} = \frac{\partial \hat{\phi}_2^1}{\partial z},\ z = h_2,\ 0 < r < R \quad (48)$$

$$\hat{\phi}_1^1 = \hat{\phi}_2^1 + \tilde{\phi}_2^1,\ z = h_2,\ 0 < r < R \quad (49)$$

$$\frac{\partial \hat{\phi}_1^1}{\partial r} = 0,\ r = R,\ h_2 < z < H \quad (50)$$

region 2

$$\nabla^2 \hat{\phi}_2^1 = 0,\ 0 < r < R,\ h_1 < z < h_2 \quad (51)$$

$$\frac{\partial \hat{\phi}_2^1}{\partial z} = \frac{\partial \hat{\phi}_1^1}{\partial z},\ z = h_2,\ 0 < r < R \quad (52)$$

$$\hat{\phi}_2^1 = \hat{\phi}_1^1 - \tilde{\phi}_2^1,\ z = h_2,\ 0 < r < R \quad (53)$$

$$\frac{\partial \hat{\phi}_2^1}{\partial z} = \frac{\partial \hat{\phi}_3^1}{\partial z},\ z = h_1,\ 0 < r < R \quad (54)$$

$$\hat{\phi}_2^1 = \hat{\phi}_3^1 - \tilde{\phi}_2^1,\ z = h_1,\ 0 < r < R \quad (55)$$

$$\frac{\partial \hat{\phi}_2^1}{\partial r} = 0,\ r = R,\ h_1 < z < h_2 \quad (56)$$

region 3

$$\nabla^2 \hat{\phi}_3^1 = 0,\ 0 < r < R,\ 0 < z < h_1 \quad (57)$$

$$\frac{\partial \hat{\phi}_3^1}{\partial z} = \frac{\partial \hat{\phi}_2^1}{\partial z},\ z = h_1,\ 0 < r < R \quad (58)$$

$$\hat{\phi}_3^1 = \hat{\phi}_2^1 + \tilde{\phi}_2^1, \quad z = h_1, \quad 0 < r < R \tag{59}$$

$$\frac{\partial \hat{\phi}_3^1}{\partial z} = 0, \quad z = 0, \quad 0 < r < R \tag{60}$$

$$\frac{\partial \hat{\phi}_3^1}{\partial r} = 0, \quad r = R, \quad 0 < z < h_1 \tag{61}$$

SOLUTIONS

For a weak plane incident pressure wave (e.g. see Arfken and Weber (2001))

$$\phi_I^0 = ae^{ik_0 r\cos\theta} = a\sum_{m=0}^{\infty}\alpha_m J_m(k_0 r)\cos m\theta, \quad \alpha_m = \begin{cases} 1, & m=0 \\ 2i^m, & m>0 \end{cases} \tag{62}$$

where a = small amplitude ($a << 1$), and the incident pressure wave comes from the direction of θ_0 as shown in Figure 2, the velocity potential may also be represented as

$$\phi_I^0 = ae^{i\vec{k}_0\cdot\vec{r}} = ae^{i[k_0 x\cos\theta_0 + k_0 y\sin\theta_0]}$$
$$= ae^{i(+k_0 r\cos\theta\cos\theta_0 + k_0 r\sin\theta\sin\theta_0)} = ae^{ik_0 r\cos(\theta-\theta_0)} = ae^{ik_0 r\cos\theta'} \tag{63}$$

Thus, the coordinate transformation

$$\theta' = \theta - \theta_0 \tag{64}$$

transforms old coordinate system ($\theta = 0$ at x axis) to the new one ($\theta' = 0$ at the direction of incident pressure wave). Without losing the generality, we will choose the new coordinate system in latter discussions.

Straightforwardly, substituting (62) into $O(1) terms$, z-independent

$$\phi_4^0 = \sum_{m=0}^{\infty} aA_m^0 H_m^{(1)}(k_0 r)\cos m\theta' \tag{65}$$

$$A_m^0 = -\frac{\alpha_m J_m(k_0 R)}{H_m^{(1)}(k_0 R)}, \quad m = 0,1,2,\ldots \tag{66}$$

is obtained.

By using (38)-(41), (62)-(63) and applying the orthogonality of trigonometric and Bessel functions, we get z-independent

$$\tilde{\phi}_2^1 = \sum_{m=0}^{\infty} a\tilde{B}_m J_m(k_0 r)\cos m\theta' \tag{67}$$

$$\tilde{B}_m = \frac{-2i\alpha_m n_0 K}{\pi k_0 R J_m'(k_0 R) H_m^{(1)}(k_0 R)}, \quad m = 0,1,2,\ldots \tag{68}$$

and trivial solutions for $\tilde{\phi}_1^1$ and $\tilde{\phi}_3^1$. Similarly, (46)-(61) together with (65) give z-dependent

$$\hat{\phi}_1^1 = \sum_{m=0}^{\infty}\sum_{n=1}^{\infty}\left[\hat{A}_{mn}\cosh(k_{mn}z) + \hat{B}_{mn}\sinh(k_{mn}z)\right]J_m(k_{mn}r)\cos m\theta' \tag{69}$$

$$\hat{\phi}_2^1 = \sum_{m=0}^{\infty}\sum_{n=1}^{\infty}\left[\hat{C}_{mn}\cosh(k_{mn}z) + \hat{D}_{mn}\sinh(k_{mn}z)\right]J_m(k_{mn}r)\cos m\theta' \tag{70}$$

$$\hat{\phi}_3^1 = \sum_{m=0}^{\infty}\sum_{n=1}^{\infty}\hat{E}_{mn}\cosh(k_{mn}z)J_m(k_{mn}r)\cos m\theta' \tag{71}$$

where k_{mn} = the wave number in the well,

$$\hat{A}_{mn} = a\Omega_{mn}\frac{A_{12}^H}{A_{11}^H}\cdot\Theta_{mn} \tag{72}$$

$$\hat{B}_{mn} = -a\Omega_{mn}\cdot\Theta_{mn} \tag{73}$$

$$\hat{C}_{mn} = a\Omega_{mn}\frac{1}{A_{11}^H}\left[A_{11}^H\cdot\cosh(k_{mn}H) + A_{12}^H\cdot\Theta_{mn}\right] \tag{74}$$

$$\hat{D}_{mn} = a\Omega_{mn}\sinh(k_{mn}h_1) \tag{75}$$

$$\hat{E}_{mn} = a\Omega_{mn}\frac{1}{A_{11}^H}\left[\omega^2\cdot\Lambda_{mn} - gk_{mn}\cdot\Gamma_{mn}\right] \tag{76}$$

$$A_{11}^H = \omega^2\cosh(k_{mn}H) - gk_{mn}\sinh(k_{mn}H) \tag{77}$$

$$A_{12}^H = \omega^2\sinh(k_{mn}H) - gk_{mn}\cosh(k_{mn}H) \tag{78}$$

$$\Theta_{mn} = \sinh(k_{mn}h_2) - \sinh(k_{mn}h_1) \tag{79}$$

$$\Lambda_{mn} = \cosh(k_{mn}(H-h_1)) - \cosh(k_{mn}(H-h_2)) \tag{80}$$

$$\Gamma_{mn} = \sinh(k_{mn}(H-h_1)) - \sinh(k_{mn}(H-h_2)) \tag{81}$$

$$\Omega_{mn} = -\frac{2in_0 K}{\pi k_0 R}\frac{\alpha_m}{J_m'(k_0 R)H_m^{(1)}(k_0 R)}\cdot\frac{\int_0^R rJ_m(k_0 r)J_m(k_{mq}r)dr}{\int_0^R rJ_m(k_{mn}r)J_m(k_{mq}r)dr} \tag{82}$$

Finally, according to (13) or (12), the perturbed wave profile is obtained as the real part of

$$\eta = \frac{i\omega\phi_1^1}{g}\varepsilon + O(\varepsilon^2) \tag{83}$$

and the non-dimensional form may be defined as

$$\frac{\eta}{a} \sim \frac{i\omega}{g}\phi_1^1\varepsilon = i\omega\cdot\sum_{m=0}^{\infty}\sum_{n=1}^{\infty}\frac{k_{mn}\cdot\Omega_{mn}\cdot\Theta_{mn}}{\cosh(k_{mn}H)\cdot\left[\omega^2 - gk_{mn}\tanh(k_{mn}H)\right]}\cdot J_m(k_{mn}r)\cos m\theta \tag{84}$$

From the denominator of the above equation, we may easily find that as

$$\omega^2 - gk_{mn}\tanh(k_{mn}H) \to 0 \tag{85}$$

where $k_{mn} = \beta_{mn}/R$; β_{mn} = specific eigenvalues of Bessel function which satisfies

$$\left.\frac{d}{d\beta}J_m(\beta)\right|_{\beta=\beta_{mn}} = 0 \tag{86}$$

the amplitude of wave height is going to be infinite and resonance thus occurs.

Notice that the order of magnitude of H is about 10 m, hence $\tanh(k_{mn}H) \to 1$; i.e. H has no effect on the occurrence of resonance practically.

RESULTS

In the following discussion, we only apply the porosity $n_0 = 0.3$ and the radius of well $R = 0.2$ m for demonstration. More detailed data are given in Table 2.

Fig. 3(a) and 3(b) show a comparison example of vertical contour distributions of perturbed velocity potential in the direction of $\theta' = 0$ in response to same incoming pressure wave with and without resonance (Fig. 3(a) for $m = 1$, $n = 2$). From top to bottom are figures near free surface, Region 1, Region 2, and Region 3, respectively. It is observed that when a weak incident pressure wave transmitting into the well through the screen, the contours of velocity potentials vary significantly and violently in the top figure of Fig. 3(a) as resonance occurs, while it is quiescent in the top figure of Fig. 3(b) as resonance does not occur. It is also observed that since both the contours of velocity potentials in Fig. 3(a) and Fig. 3(b) are discontinuous near the place of $z \cong 20$ m, the incident pressure wave cannot cause resonance on free surface directly. We thus conclude that the weak pre-earthquake longitudinal pressure wave only plays the role as a trigger to disturb the initial equilibrium state of water in the well, while the main driving mechanism for resonance of transverse free surface water wave is still the gravitational force. Notice that since the radius of observing well is so small, huge energy to disturb the equilibrium of well water is not necessary. In summary of Fig. 3, a weak pre-earthquake longitudinal pressure wave is only a triggering mechanism for the resonance of transverse gravitational free surface water wave inside the well.

Because when a specific mode of resonance occurs, the amplitude of water elevation of the corresponding mode tends to be infinite, while that of other modes are small and negligible, we thus can rewrite the series representation (84) to reveal a specific mode of resonance as

$$\frac{\eta_{mn}}{a} \sim \frac{i\omega k_{mn} \cdot \Omega_{mn} \cdot \Theta_{mn}}{\cosh(k_{mn}H) \cdot \left[\omega^2 - gk_{mn} \tanh(k_{mn}H)\right]} \cdot J_m(k_{mn}r) \cos m\theta' \qquad (87)$$

Further, the non-dimensional water elevation (87) of a specific mode of resonance multiplied by $\left[\omega^2 - gk_{mn} \tanh(k_{mn}H)\right]$ can be used not only to avoid singular behavior of (87) but also to reveal the wave pattern clearly on the other hand. Fig. 4 presents the wave pattern of surface water when resonance occurs. From top to bottom, figures of $m = 0,1,2$ are shown in Fig. 4. Fig. 4(a) is for $n = 2$, while Fig. 4(b) is for $n = 3$. It is observed that when m equals zero, the pattern of water elevation is axisymmetric and is independent of θ'. However, when m doesn't equal zero, the water elevation will have θ'-dependence, and the resonance wave pattern has plane-symmetry with m-symmetric planes as $\theta' = \frac{2j\pi}{m}$ ($j = 0,1,\ldots,m-1$).

The symmetric plane of resonance wave pattern of $m = 1$ provides a method to determine the direction of incoming pressure wave as indicated by Fig. 4. Therefore, the symmetric plane of resonance wave pattern of $m = 1$ can be used to point out the direction between the well and the location that pre-earthquake occurs. For practical application, based on this property, the location of possible later earthquake source can be determined by intersecting the direction-lines of several observing wells at different positions provided that the observing time-interval is in the order of seconds because the time periods of most earthquakes are in seconds.

CONCLUSIONS

The physical phenomenon of resonant amplification of free surface water wave in well in response to weak pre-earthquake longitudinal pressure wave transmitting through confined aquifer is analyzed successfully in the present study.

In solving this problem, a regular perturbation expansion method based on a small gauge function $\varepsilon = k_0 R$ is introduced to overcome the conventional difficulty that arose from the small value of K appearing in continuous mass flux boundary condition on the well screen, (19).

Instead of resonance of water surface in the well induced by huge longitudinal pressure wave as Cooper et al. (1965) which being similar to water oscillation in U-tube, and resonance of water surface wave induced by huge incoming transverse wave flux as traditional harbour resonance, in the study, we get a different mechanism of resonance. It is a resonance of transverse free surface water wave inside the well of small radius triggered by a weak pre-earthquake incoming longitudinal pressure signal transmitting through the confined aquifer.

The symmetric plane of resonance wave pattern of $m = 1$ can be used to point out the direction between the well and the location that pre-earthquake occurs. For practical application, based on the aforementioned property, the location of possible later earthquake source can be determined by intersecting the direction-lines of several observing wells at different positions provided that the observing time-interval is in the order of seconds because the time periods of most earthquakes are in seconds.

ACKNOWLEDGEMENTS

This study is sponsored by the National Science Council of R.O.C, under grant NSC95-2221-E-002-420.

REFERENCES

Arfken, G. B., and Weber, H. J. (2001), *"Mathematical Methods for Physicists"*, 5th ed, Harcourt Sci. and Tech. Co.

Biot, M. A. (1962), "Mechanics of deformation and acoustic propagation in porous media", *J. Appl. Phys*., 33, 1482-1498.

Chen, H. S., and Mei, C. C. (1974), "Oscillations and wave forces in an offshore harbor", Ralph M. Parsons Laboratory, Report NO.190, MIT.

Cooper, H. H., Bredehoeft, J. D., Papadopulos, I. S., and Bennett, R. R., (1965), "The response of well-aquifer systems to seismic waves", *J. Geophys. Res.*, Vol. 70, 3915-3926.

Huang, L. H., and Song, C. H. (1993), "Dynamic response of poroelastic bed to water waves", *J. Hydraulic Engineering, ASCE*, Vol. 119, 1003-1020.

Lee, J. J. (1969), "Wave-induced oscillations in harbours of arbitrary shape", Report KH-R-20, W. M. Keek Laboratory of Hydraulics and Water Resources, CIT.

Liu, L. F., and Wen, J. G. (1997), "Nonlinear diffusive surface waves in porous media", *J. Fluid Mech*., Vol. 347, 119-139.

McNown, J. S. (1952), "Waves and seiche in idealized ports", *Gravity Wave Symposium*, National Bureau of Standards Circular 521.

Mei, C. C. (1989), *"The applied dynamics of ocean surface waves"*, World Scientific Publishing Co. Pte. Ltd.

Streeter, V. L. and Wylie, E.B. (1987), *"Fluid Mechanics"*, 8th ed., McGraw-Hill, Inc.

Tsay, T. K. and Liu, P. L-F. (1983), "A finite element model for wave refraction and diffraction", *Appl. Ocean Research*, Vol. 5, 30-37.

Table 1. Schematic diagram of solving sequence

Inside the well ϕ		Outside the well Φ
—		$O(1)$
$O(\varepsilon)$	⇠ →	$O(\varepsilon)$
$O(\varepsilon^2)$	⇠ →	$O(\varepsilon^2)$
⋮		⋮
⋮		$O(\varepsilon^{n-1})$
$O(\varepsilon^n)$	⇠ →	$O(\varepsilon^n)$
⋮		⋮

⇢ Flux transport
→ Pressure transport

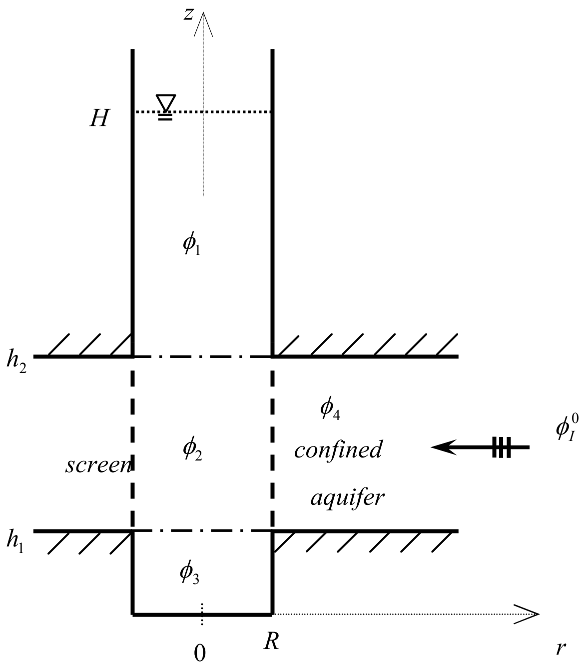

Figure 1. Schematic diagram of weak incident pressure wave impacting on a well in side view.

Table 2. Detailed data of each variable used in this study

Variable	Notation	Value	Unit
Density of fluid	ρ	1000	kg/m^3
Hydraulic conductivity	K	0.001	m/s^2
Gravitational acceleration	g	9.81	$kg \cdot m/s^2$
Radius of well	R	0.200	m
Water depth in well	H	50.0	m
Height of the lower confined aquifer boundary	h_1	1.0	m
Height of the upper confined aquifer boundary	h_2	10.0	m
Porosity	n_0	0.300	

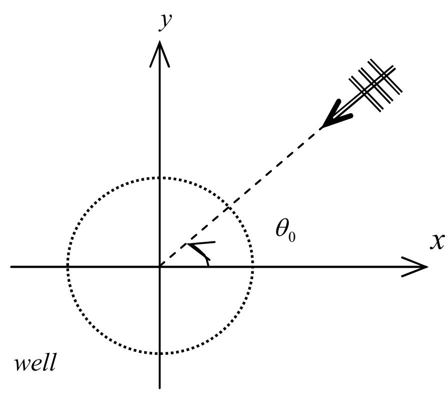

Figure 2. Schematic diagram of weak incident pressure wave impacting on a well in top view.

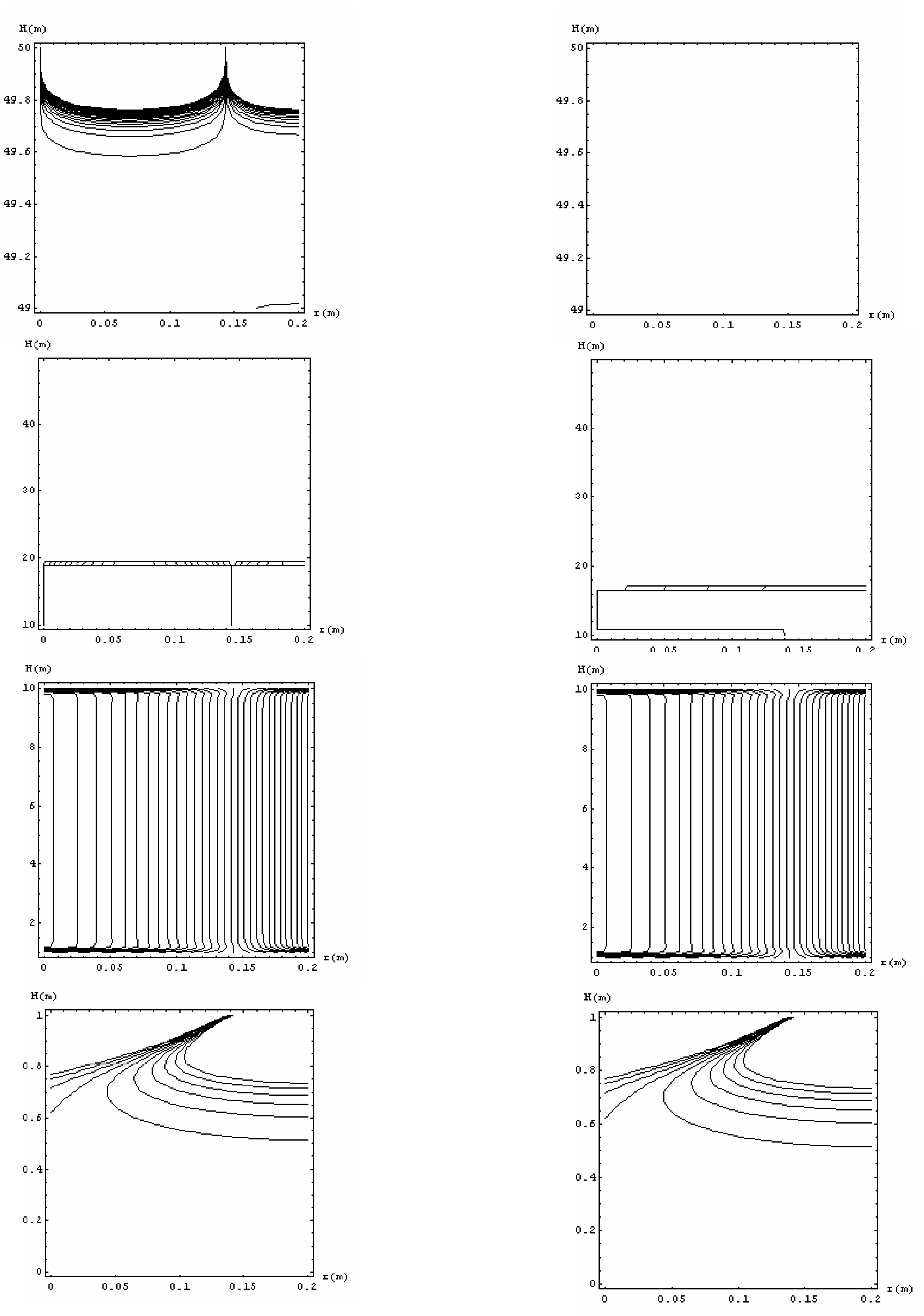

(a) (b)

Figure 3. Contour distributions of perturbed velocity potential in the direction of $\theta' = 0$: (a) with resonance (b) without resonance

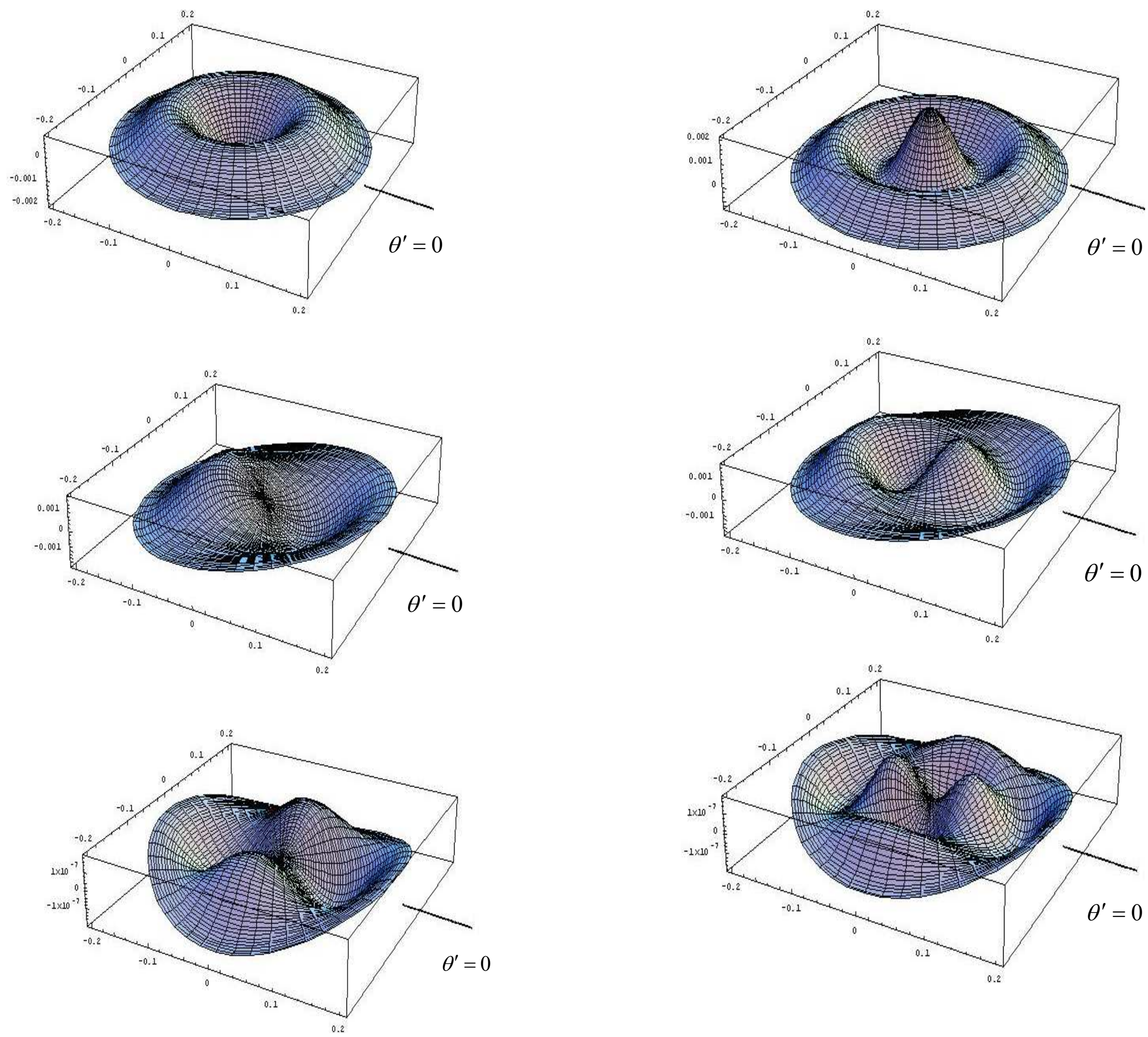

(a) (b)

Figure 4. Resonance wave pattern of surface water when resonance occurs for each resonance parameter: (a) $n = 2$ (b) $n = 3$